Available online at www.sciencedirect.com
SCIENCE DIRECT®

Journal of Photochemistry and Photobiology A: Chemistry 177 (2006) 191–196

Journal of Photochemistry and Photobiology A:Chemistry
www.elsevier.com/locate/jphotochem

Preparation of initiator and cross-linker-free poly(*N*-isopropylacrylamide) nanogels by photopolymerization

Qiao Xiangli[a,*], Zhang Zhenjia[a], Yao Side[b]

[a] *Environmental Science and Engineering Department, Shanghai JiaoTong University, Shanghai 200240, China*
[b] *Shanghai Research Institute of Applied Physics, Shanghai 200240, China*

Received 12 April 2005; received in revised form 9 May 2005; accepted 30 May 2005

Abstract

Poly(*N*-isopropylacrylamide) or PNIPAm nanogels with diameter of 50–200 nm were prepared from *N*-isopropylacrylamide monomer by photopolymerization in the absence of initiator, cross-linker and surfactant. Morphology transition of the nanogels from branch to compact, global one was tuned with NIPAm(*N*-isopropylacrylamide) concentration in reaction. Reaction mechanism of the nanogels formation was proposed. The yield of prepared nanogels can increased from ca. 20 up to 86% when solution pH varied from neutral to 2. ESR signals confirmed that the existence of H^+ in reaction could accelerate the polymerization of NIPAm.

Keywords: Poly(*N*-isopropylacrylamide) nanogels; Photopolymerization; Crosslinker-free; Morphology transition; ESR

1. Introduction

Temperature-responsive particles with a submicrometer size range have found wide application in the fields of life science and technology [1–3], such as controlled-release drug delivery, degradable medical materials [4–8], etc. Of these thermo-responsive polymers, PNIPAm maybe is the most intensively studied polymer, which has a sharp phase transition around 32 °C, lower critical solution temperature (LCST). Below LCST, it is in a swollen state, containing a large amount of water. When temperature is increased above LCST, polymer chains collapsed and water molecules dissociated from it rapidly. A large number of PNIPAm hydrogels were prepared by photopolymerization, emulsion or precipitation polymerization [9–12], etc. These methods usually contained monomer and initiator. Chemical cross-linker is usually employed in order to produce highly cross-linked polymers. PNIPAm hydrogels prepared by these ways usually have a large volume, and will be cut into small disks to study their thermodynamics or volume phase transition in response to environmental stimulus [13].

Polymeric particles size and size distribution have a strong influence on its application [14,15]. For example, as a drug delivery carrier, the desired diameter of responsive hydrogels are in 20–100 nm range [16,17]. Furthermore, the purity of the drug carrier is required to be high. However, in most literatures, chemical cross-linker, initiator, and surfactant (usually SDS) are always employed in polymerization system to prepared PNIPAm micro- or nanogels particles [18–20]. It is known that the existence of cross-linker can lead to structural inhomogeneities which will harm phase transition rate of hydrogels towards environmental stimulus [21–23], as reaction rate of cross-linker is different from that of the monomer [24]. Recently, Gao et al. [25] synthesized PNIPAm nanogels with hundreds of nanometers initiated by Potassium persulfate (KPS) without the addition of cross-linker and surfactants. The formation of nanospheres was attributed to self-cross-linking of polymer chains.

Of these methods mentioned above, photopolymerization maybe the simplest way to prepared homogeneous highly cross-linked PNIPAm hydrogels [26]. However, the

---

[*] Corresponding author. Tel.: +86 21 54747412; fax: +86 21 54745640.
E-mail address: qiao_xl@sjtu.edu.cn (Q. Xiangli).

1010-6030/$ – see front matter © 2005 Elsevier B.V. All rights reserved.
doi:10.1016/j.jphotochem.2005.05.025

monomers employed are multifunctional ones. Furthermore, photosensitive initiator is always introduced into reaction mixture in order to obtain highly cross-linker polymer hydrogels [27]. In our paper, we report the polymerization of PNIPAm nanogels with diameter of 50–200 nm from NIPAm monomer (mono-functional monomer) initiated directly with UV in the absence of added initiator, cross-linker and surfactants. The advantages of this report is that the system is simple and the purity of the produced nanogels is high which has a great potential application in medical field. Morphology transition of the prepared nanoparticles from branch to global are visualized by SEM. The yield of prepared nanoparticle (w/w, nanoparticle weight/monomer weight) can be improved up to ca. 86% at pH 2 from ca. 20% in neutral solution. ESR signals show that more free radicals were generated in low pH solution, comparing with that in high one which indicates that the existence of H^+ accelerates the photopolymerization of PNIPAm. Mechanism of PNIPAm nanoparticle formation is proposed.

2. Experimental/materials and methods

2.1. Materials

N-Isopropylacrylamide was purchased from Tokyo Kasei Ltd., and purified by recrystallization from hexane before use. Three-distilled deionized water are used for the aqueous solution polymerization. Other reagents used were analytical grade. Sulfonated polyethersulfone (SPES) membranes (its molecular weight cut off value being 5 kD) were purchased from Membrane Research Center of Shanghai Research Institute of Applied Physics to remove unreacted monomers from PNIPAm solution.

2.2. Photo-polymerization of PNIPAm nanogels

The polymerization procedure of PNIPAm nanogels are conducted as follows: a mixture of NIPAm monomer and distilled water of variable ratios is dispersed with a two-blade stirrer at 200 rpm in a 50 mL four-neck quartz flask. The reaction mixture is kept at 30 °C under the stream of N_2 for 30 min. Upon the illumination of a 500 W Xe lamp (details of the reaction condition is described in next paragraph), the polymerization is carried out at 30 °C for 5 h under a N_2 atmosphere. As the illumination light is weak, there is no obvious temperature change during polymerization. Finally, the PNIPAm nanogels particles are purified by using sulfonated polyethersulfone (SPES) membrane (its molecular weight cut off value being 5 kD) to remove unreacted monomers. pH of the solution was tuned by adding different amount of 0.2 mol/L HCl or 0.1 mol/L HCl aqueous solution.

The scheme of this photopolymerization equipment setup is presented in Fig. 1. Its reaction condition is as follows: The distance was set at 24 cm with a convex placed between reaction quartz flask and Xe-lamp. Upon the illumination of Xe-lamp, ray light from it penetrates through a rounded hole (ca. 1.54 cm^2 area) which has a ca. 2 cm distance to lamp, then it is converged through a quartz convex at quartz flask to initiate the mixture solution being agitated with a magnetic heater stirrer. A color filter is placed between quartz convex and reaction flask to eliminate rays whose wavelength ≥500 nm as monomer has little absorptance of theses rays (UV–vis absorptance of monomer was shown in Fig. 2).

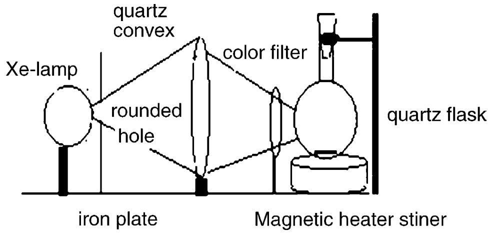

Fig. 1. Schematic of photopolymerization equipmental setup.

2.3. Characterization of the prepared PNIPAm nanogels

The prepared PNIPAm nanogels were characterized mainly by scanning electron microscope (SEM), ^{1}H-nuclear magnetic resonance (^{1}H NMR), photon correlation spectroscopy (PCS). For SEM ananlysis, 3×10^{-2} mg/mL PNIPAm nanogels are dropped on 10 mm^2 surface of silicon wafer. Dried the samples in a vacuum drier overnight. The morphologies of the prepared PNIPAm nanogels are detected by scanning electron microscope (SEM) LEO 1350 VP (Germany) employed at 5–10 kV. Chemical structures of these nanogels are measured by ^{1}H NMR techniques. Samples for ^{1}H NMR are prepared as follows: dried the PNIPAm nanogels particles under vacuum pressure, then dissolves it in D_2O solvent. Its spectra is recorded on a Bruker NMR Spectrometers:

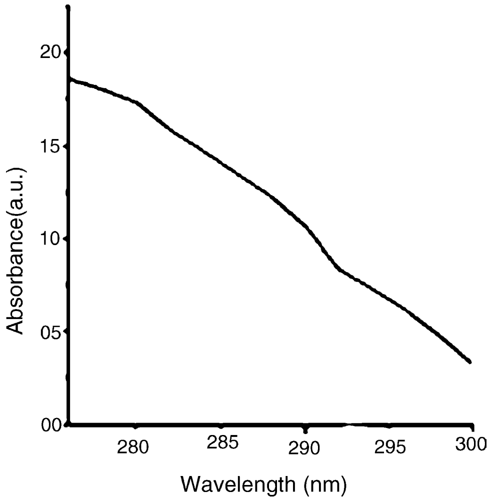

Fig. 2. Absorption spectrum of NIPAm in water.

avance DmX-500 at 25 °C. The sizes of PNIPAm nanogels are detected by photon correlation spectroscopy (PCS) Zeta-Sizer 3000HS (Malvern Instrument Ltd.) fitted with a 5 mV He–Ne laser (Ï) 633 nm. Data are taken at an angle of 90° and at a temperature of 25 °C. Electron spinning resonance (ESR) apparatus is used to detect free radicals present in aqueous solution. The ESR signals are detected on-line. The intensities of ESR signals can be compared with each other to determine the amount of free radicals generated in different reaction mixture. A mixture of NIPAm and water is put into a quartz tube with inner, outer diameter and length being 2, 2.5 mm, and 22 cm respectively. Then immersed it in liquid nitrogen. Under the protection of liquid nitrogen, the tube is placed into test cavity. Upon illumination of a 500Xe-lamp on quartz tube for 30 min, the ESR signals are measured on a VIRIAM E112 (US) 100 kHz magnetic field. ESR spectrometer settings were as follows: modulation amplitude, 4 G; time constant, 0.064 s; microwave power, 1 mW and receiver gain, 4e4.

3. Results and discussion

3.1. Synthesis of PNIPAm nanogels by UV

NIPAm monomer has a strong and abroad UV absorption around 270 nm wavelength, as shown in Fig. 2. The curve of UV–vis absorption versus wavelength for NIPAm monomer is measured on a UV–vis spectrometer (Perkin-Elmer, Lambda 900). For photopolymerization of most multifunctional monomers, a photosensitive initiator is always needed in reaction mixture, as the monomers can not generate sufficiently reactive species directly irradiated by UV. Furthermore, these photosensitive initiators are expensive in some cases. However, in our system, we found that NIPAm monomer in water can be directly initiated with UV to polymerize leading to the formation of nanogels particles in the absence of initiator, cross-linker and surfactant. NIPAm monomer concentration within 5×10^{-2} and 9×10^{-1} mol/L range has a strong influence on morphology of the prepared nanoparticles. Following we will discuss this in detail.

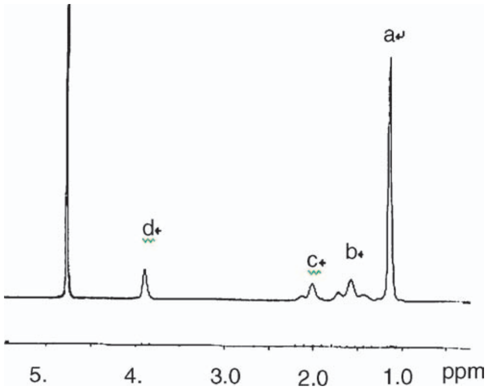

Fig. 3. ^{1}H NMR spectrum of the prepared PNIPAm nanogel particles.

3.2. The influence of NIPAm monomer concentration on the prepared PNIPAm nanogels

^{1}H NMR spectra of the prepared nanoparticles is presented in Fig. 3 (samples are prepared following the procedure described above. In Fig. 3, Peaks a–d are assigned as $-C\underline{H}_3$, 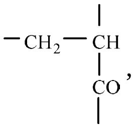 $-CH_2-\overset{|}{\underset{\underset{\underset{|}{CO}}{|}}{CH}}$, 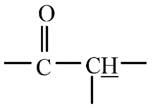 $-\overset{\overset{O}{\|}}{C}-\underset{|}{C\underline{H}}-$, and 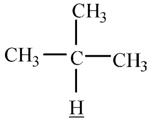 $CH_3-\overset{\overset{CH_3}{|}}{\underset{\underset{\underline{H}}{|}}{C}}-CH_3$ protons, respectively. Peak c of 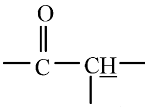 $-\overset{\overset{O}{\|}}{C}-\underset{|}{C\underline{H}}-$ (2.0 ppm) in Fig. 3 demonstrates that NIPAm monomer in solution has been transformed into PNIPAm polymer under the irradiation of UV ray.

During the experiments, it is found that morphology of the nanoparticles is greatly affected by initial monomer concentration in solution. Fig. 4 shows a series of SEM images of PNIPAm nanogel particles prepared in water solution. Parts a–d demonstrates that morphology transition of PNIPAm nanoparticles from highly branched nanogels to hard global nanospheres is clearly visible, which is formed in 5.53×10^{-2}, 9.06×10^{-2}, 7.08×10^{-1}, and 9.08×10^{-1} mol/L NIPAm solution, respectively.

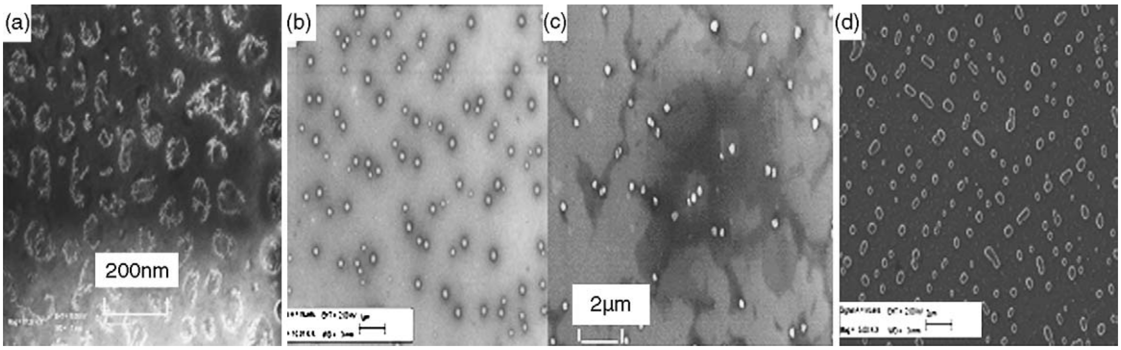

Fig. 4. SEM images demonstrating the effect of initial monomer concentration on preapred PNIPAm nanoparticles. (a) $C_{\mathrm{NIPAm}} = 5.53 \times 10^{-2}$ mol/L; (b) $C_{\mathrm{NIPAm}} = 9.06 \times 10^{-2}$ mol/L, the scale bar being 1 µm; (c) $C_{\mathrm{NIPAm}} = 7.08 \times 10^{-1}$ mol/L; (d) $C_{\mathrm{NIPAm}} = 9.08 \times 10^{-1}$ mol/L, the scale bar being 2 µm.

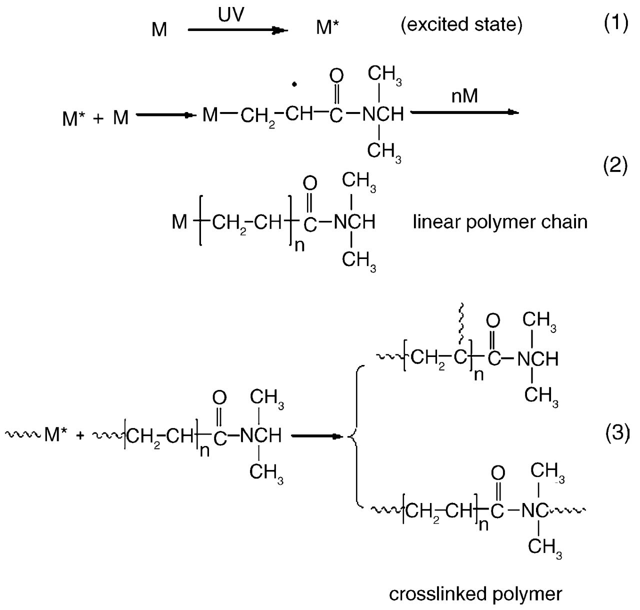

Fig. 5. Reaction mechanism of PNIPAm nanogels formation under the irradiation of UV.

We attributed the morphology transitions of the resulting PNIPAm nanogels to different diffusion rates of monomer or oligomer to reactive species through the polymerization. As discussed above, NIPAm monomer can be directly initiated to polymerize into PNIPAm upon its exposure to UV. In other words, NIPAm molecules can be directly excited to higher energy state with UV, where they either react with vinyl group of NIPAm to continue the reaction resulting in linear polymer chain, or/and abstract atom H from another NIPAm molecule, oligomer or macromolecule to proceed the polymerization, leading to the formation of a branch polymer [28] (as demonstrated in Fig. 5). There are two most reactive H atoms in NIPAm chain [25]: one is on the *tert*-C of the pendant isopropyl group and the other is in the main chain backbone. These active H atoms are likely to be attacked by excited state monomer, forming *tert*-C free radicals to continue the polymerization (see equation [3] in Fig. 5). Free radicals in solution may be terminated with macromolecular free radicals, oligomer, or chain transfer. All these possible reactions produce the cross-linked PNIPAm nanogels. The reaction mechanism of PNIPAm nanogels formation are demonstrated below in Fig. 5 (M represent monomer 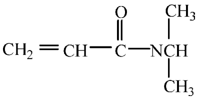 $CH_2{=}CH{-}C({=}O){-}NCH(CH_3)_2$).

In dilute solution containing less monomer, polymerization proceeds in two stages [29]: oligomer formation and intermolecular reaction between oligomers. Oligomers formed in this case mainly result from the reactions among free radicals generated from vinyl groups under the irradiation by UV, as vinyl groups are more easily attached by reactive species. When vinyl groups are consumed to some degree, reactive species produced from *tert*-C play a predominant role, therefore inter-oligomer reaction occurs leading to the possibility of a cross-linking network. However, the amount of produced oligomer is far from enough, so, there is only a limited degree of cross-linking reaction takes place among oligomers, as most free radicals vanish before they collide with oligomer or others, resulting in the formation of branch nanogels which is stabilized by swollen chains from surface of the nanogels.

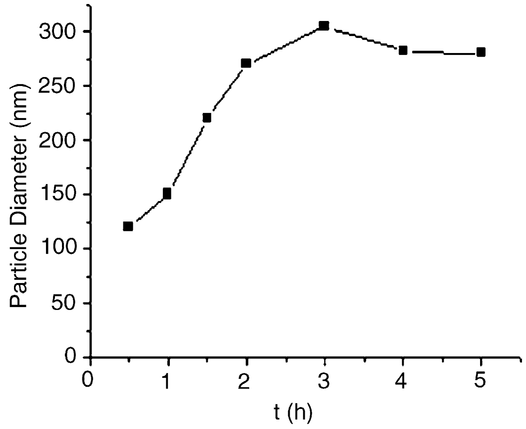

Fig. 6. Particle diameter variation with reaction time *t* (h) in solution containing 9.08×10^{-1} mol/L monomer concentration.

As monomer concentration increasing, more free radicals per volume are generated in solution. Simultaneously, amount of *tert*-C free radicals also increase up to a value which can effectively initiate the monomers or oligomers to react, thus forming a relatively high cross-linked nanoparticles. Diameter of the produced nanoparticles continue to grow until the monomers or oligomers consumed to some degree where they don't have enough time to dissipate to reactive species before the distinguish of free radicals. So, cross-linking reaction become more difficult with time on. Thus, the NIPAm nanoparticles produced are expected to possess a relatively dense cross-linked core with loosely cross-linking shell, whose swollen state in water prevent them from aggregating.

This assumption of polymerization process can be explained with diameter variation of produced nanoparticles (see in Fig. 6) in solution containing 9.08×10^{-1} mol/L monomer as measured with photon correlation spectroscopy (PCS) ZetaSizer 3000HS (Malvern Instrument Ltd.).

From Fig. 6, we can see that at initial stage of polymerization, large variation in particles diameter from ca. 120–150 nm within 0.5 h takes place, then increases rapidly with reaction time up to its maximum value ca. 300 nm, finally, to ca. 280 nm with slightly reduction in diameter, comparing with 300 nm at 3 h. This curve demonstrates that immediate precursors to nanoparticles are generated from monomers at first stage of polymerization. Then a more rapidly increase in particle diameter is caused by inter-cross-linking among these precursors. When monomer and immediate precursors are consumed, intra-cross-linking in macrogels prevails, forming cross-linked nanoparticles, with

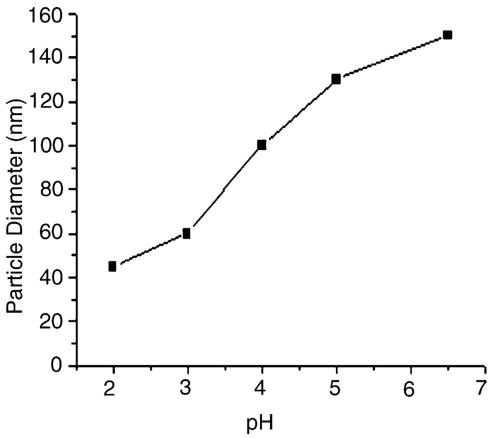

Fig. 7. Nanoparticle diameter variation with pH in solution containing 5.53×10^{-2} mol/L NIPAm.

a little shrinkage in diameter comparing with its maximum diameter, ca. 300 nm, due to high cross-linking density inside nanoparticles.

3.3. Influence of solution pH on the prepared PNIPAm nanogels

All experiments discussed above are completed in neutral solution, whereas, low monomer conversion to nanoparticles is observed after 5 h polymerization in solution, whose nanoparticle yield is ca. 20% in solution with 5.53×10^{-2} mol/L monomer concentration. But its yield can be greatly improved up to 86% when pH value is decreased to 2. pH variation in solution can also strongly affect sizes of the nanoparticles. Curve of diameter of prepared PNIPAm nanoparticles with pH solution is illustrated in Fig. 7 (initial monomer concentration is fixed at 5.53×10^{-2} mol/L).

When monomer concentration is fixed at 5.53×10^{-2} mol/L, the nanoparticle volume decreases rapidly with decreasing of pH till down to ca. 45 nm at pH 2, whereas, its polymer yield is dramatically enhanced to 86%. This suggested that H^+ in solution has an accelerating function on PNIPAm nanoparticle formation. It is known that the existence of H^+ can improve solvability of the solution, which cause NIPAm molecule or oligomer to rearrange its configuration. With the decrease of pH, monomers or oligomers tend to form smaller, compact micells (see b in Fig. 8), with hydrophobic part, $CH_2{=}CH_2$–, inner the micell; while hydrophilic part, 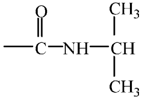 $-\overset{\overset{\displaystyle O}{\|}}{C}-NH-\underset{\underset{\displaystyle CH_3}{|}}{\overset{\overset{\displaystyle CH_3}{|}}{CH}}$, spreading outside towards solution. Upon the start of photolpolymerzation, the micells structure begins to form, then fixes, finally cross-linked. The remaining monomers in solution consumed in a mode as discussed above. The scheme of micell formation is presented as Fig. 8.

Thus, the formation of higher density crosskined nanoparticles are expected at lower pH solution on the basis of mechanism proposed in Section 3.2. This assumption is confirmed by SEM image of PNIPAm nanoparticles prepared from 9.08×10^{-2} mol/L monomer solution at pH 2 which has a smooth global surface with a relative higher density (see Fig. 9), comparing with branch nanogels obtained under the same condition except in neutral solution (see part a in Fig. 4). The expectation is also confirmed at high monomer concentration, 9.08×10^{-1} mol/L in pH 2 aqueous solution. Its nanoparticle yield is ca. 89%, while its corresponding size is ca. 5 nm (PCS data). However, with the increasing of monomer concentration, viscosity of reaction mixture increases rapidly with polymerization process making agitation become very difficult.

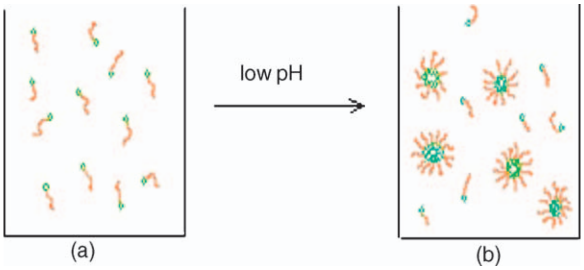

Fig. 8. Scheme of micell formation in low pH solution. °, Represent hydrophobic part of monomer or oligomer; ∼, represent hydrophilic part of monomer or oligomer.

ESR signals also approves the accelerating function of H^+ on the photopolymerization (see Fig. 10), which are conducted online at 77 K temperature as described above comparing curve a with b, we can deduce that more free radicals are generated in low pH solution (pH 2)than that in neutral one (these two systems conduct polymerization under the same condition with exception of pH difference).

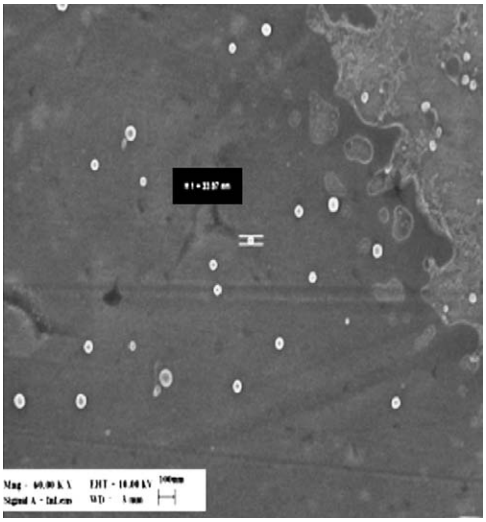

Fig. 9. SEM image of PNIPAm nanogels prepared from 9.08×10^{-2} mol/L monomer concentration solution at pH 2, the scale bar being 100 nm.

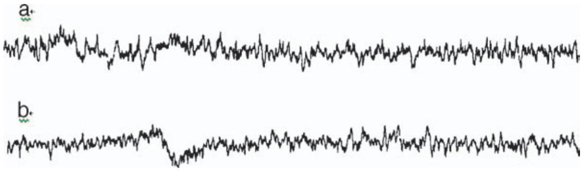

Fig. 10. ESR signals detected in reactions. Curve a represent ESR signal measured from neutral medium; b represent ESR signal measured from solution pH 2.

4. Summary

PNIPAm nanoparticles with diameters ranging from 50 to 300 nm were obtained by photopolymerization in the absence of initiator, cosslinker and surfactant in water. Morphology transition of the prepared nanopartilces from branch to compact global can be tuned with monomer concentration in reaction. This was attributed to different dissipation rates to reactive species of these monomer or oligomer which determine cross-linking degree of nanoparticles. The yield of nanoparticle is greatly improved from ca. 20% at neutral solution up to ca. 86% when pH solution is lowered to 2. Correspondingly, its morphology is shifted from branch to compact, global one. ESR signals confirms the accelerating function of H^+ to the photopolymerization of PNIPAm.

Acknowledgments

The author is grateful to Mr. Ping Z.H. of Fudan University for his assistance in ^1H NMR experiments. The present work was supported by Municipal Committee of Science and Technology of Shanghai under Grant No. 0243nm027.

References

[1] J.L. Heung, N. Yasuhide, M. Takehisa, Macromolecules 32 (1999) 6989–6995.
[2] S. Ivan, H.F. Theodore, S. Roger, M. Egon, Langmuir 16 (2000) 9031–9034.
[3] C.W. Kuo, J.Y. Shiu, P. Chen, Chem. Mater. 15 (2003) 2917–2920.
[4] T. Bettinger, J.S. Remy, P. Erbacher, Bioconjugate Chem. 10 (1999) 558–561.
[5] Q. Cai, Y.L. Zhao, J.Z. Bei, F. Xi, S.G. Wang, Biomacromolecules 4 (2003) 828–834.
[6] S. Zhou, B. Chu, J. Phys. Chem. B 102 (1998) 1364–1371.
[7] H. Senff, W. Richtering, Colloid Polym. Sci. 278 (2000) 830–832.
[8] E. Daly, B.R. Saunders, Langmuir (2000) 5546–5552.
[9] M. Annaka, T. Matsuura, M. Kasai, T. Nakahira, Y. Hara, T. Okano, Biomacromolecules 4 (2003) 395–403.
[10] J.D. Debord, L.A. Lyon, Langmuir (2003) 1–5.
[11] P.W. Zhu, D.H. Napper, Langmuir 16 (2000) 8543–8548.
[12] H. Hang, A.I. Cooper, Chem. Mater. 14 (2002) 4017–4020.
[13] X.Z. Zhang, J.T. Zhang, R.X. Zhuo, C.C. Chu, Polym. Commun. 43 (2002) 4823–4827.
[14] S. Vinogradov, E. Batrakova, A. Kabanov, Colloid Surf. B: Biointerf. 16 (1999) 291–295.
[15] R. Esfand, D.A. Tomalia, Drug Discov. Today 6 (2001) 427–432.
[16] S. Stolnik, L. Illum, S.S. Davis, Adv. Drug. Del. Rev. 16 (1995) 195–198.
[17] A.E. Hawley, S.S. Davis, L. Illum, Adv. Drug. Del. Rev. 17 (1995) 129–133.
[18] C.D. Jones, L.A. Lyon, Macromolecules 33 (2000) 8301–8306.
[19] D.J. Gan, L.A. Lyon, J. Am. Chem. Soc. 123 (2001) 7511–7515.
[20] J.P. Wang, D.J. Gan, L.A. Lyon, M.A. El-Sayed, J. Am. Chem. Soc. 123 (2001) 11284–11289.
[21] T. Norisuye, N. Masui, Y. Kida, D. Ikuta, E. Kokufuta, S. Ito, S. Panyukov, M. Shibayama, Polymer 43 (2002) 5289–5293.
[22] A. Guillermo, J.P. Cohen Addad, J.P. Bazile, D. Duracher, A. Elaissari, C. Pichot, J. Polym. Sci., Part B: Polym. Phys. 38 (2000) 889–893.
[23] A. Fernandez-Barbero, A. Fernandez-Nieves, I. Grillo, E. Lopez-Cabarcos, Phys. Rev. E 66 (2002) 803–806.
[24] X. Wu, R.H. Pelton, A.E. Hamielec, D.H. Woods, W. McPhee, Colloid Polym. Sci. 272 (1994) 467–472.
[25] J. Gao, B.J. Frisken, Langmuir 19 (2003) 5212–5216.
[26] S.P. Pappas, UV-Curing Science and Technology, vols. 1–2, Technology Marketing Corporation, Stamford, CT, 1985.
[27] C. Decker, Acta Polym. 45 (1994) 333–336.
[28] P.J. Flory, Principles of Polymer Chemistry, Cornell University Press, New York, 1953.
[29] R.S. Frank, J.S. Downey, K. Yu, H.D.H. Stover, Macromolecules 35 (2002) 2728–2735.